Study on nanocrystalline dual phase Ni–Co alloy with high strength and excellent ductility

W. C. Xu[1], P. Q. Dai*[1], X. L. Wu[2] and D. Tang[1]

In the present study, the room temperature mechanical properties of nanocrystalline Ni and Ni–75 wt-%Co alloy, prepared by pulse electrodeposition, were contrasted. Both higher strength and higher ductility were obtained for the Ni–75%Co alloy with a dual phase structure and an average grain size of 7·2 nm. By means of TEM observations of grain structures before and after tensile deformation for Ni and Ni–75%Co samples, a link between the ductility and the variation of stress induced grain growth during tensile deformation was established. Observations of TEM showed stress induced grain growth during tensile deformation, subjected to very high stresses and large strains, is very insignificant for the Ni–75%Co alloy in sharp contrast to the significant stress induced grain growth occurring in Ni. It was proposed that suppression of stress induced grain growth during tensile deformation can delay and even prohibit formation of shear banding plastic instability and thus enhances uniform strain leading to an enhanced ductility.

Keywords: Nanocrystalline, Ni–Co, Mechanical property, Tensile ductility, Grain growth, Dual phase structure

Introduction

Nanocrystalline (NC) grains are thermodynamically metastable. It is established that annealing at low temperatures can cause abnormal grain growth in many NC metals.[1] In addition to the thermal activation, grain growth induced by applied stresses at room temperature (RT),[2–10] even at cryogenic temperatures,[8,9] has also been observed in NC metals.

For NC metals, shear banding is a common type of plasticity instability. Shear bands are frequently observed on the surface of specimen, when plasticity instability occurs in the deformation process of NC metals.[11–13] Inside shear bands, it is the presence of severely deformed grains, such as elongated grains and grown grains.[13] However, the grains in the exterior of shear bands show a relatively small change in the grain size and shape.[13] On this basis, it is logical that the shear bands caused by localised deformation might firstly initiate in the region where nanograins are experiencing fast growth driven by stresses. Accordingly, we are motivated to consider a new issue: whether shear banding plasticity instability would be prohibited or delayed to enhance the ductility in NC metals, if stress induced grain growth during tensile deformation could be suppressed.

Stress induced grain growth in NC metals is due to grain boundary (GB) migration[14,15] and/or grain rotation during deformation.[2,3] Soer and co-workers gave a convincing example indicating that solutes in the matrix can pin GBs and then restrict high angle GBs' migration during deformation.[16] In a recent molecular dynamic (MD) simulation, it was predicted that GB migration was entirely suppressed in an NC Al–3 wt-%Pb alloy with a dual phase (DP) structure.[17] In the present study, the authors select a contrast experiment between electrodeposited NC Ni and an electrodeposited NC DP Ni–Co alloy to check the relationship between the variation of tensile stress induced grain growth and the ductility.

Experimental procedure

In the present study an aqueous sulphamate based electrolyte was used to produce NC Ni and an NC DP Ni–Co alloy by square wave pulse electodeposition. The electrolyte was made of $1{\cdot}65 \pm 0{\cdot}01$M total $[Ni^{2+}]+[Co^{2+}]$ ($[Co^{2+}]=0$M for Ni and $[Co^{2+}]/[Ni^{2+}]=4:6$ for the DP Ni–Co alloy), 20 g L^{-1} $NiCl_2.6H_2O$, 30 g L^{-1} boric acid, 2·5 g L^{-1} soluble saccharin and 0·1 g L^{-1} lauryl sodium sulphate. The main electrodeposited conditions are listed in Table 1. Under these conditions, NC metals, the thickness of which was 180–200 μm, were deposited on stainless steel substrates, which had been polished to a mirror-like finish surface before electrodeposition. After electrodeposition, the deposits can be mechanically stripped from stainless steels.

The composition of NC DP Ni–Co alloy was determined by the energy dispersive X-ray (EDX) spectroscopy method and the DP structure was verified by X-ray diffraction (XRD). XRD was carried out on a Philip X' Pert Pro MPP X-ray diffractometer using Cu K_α radiation. The microstructures of NC metals were

[1]College of Materials Science and Engineering, Fuzhou University, Fuzhou, 350108, China
[2]State Key Laboratory of Nonlinear Mechanics, Institute of Mechanics, Chinese Academy of Sciences, Beijing, 100080, China

*Correspondence author, email pqdai@126.com

Published by Maney on behalf of the Institute
Received 4 June 2009; accepted 27 July 2009
DOI 10.1179/026708309X12506933873224

observed by the TEM. Observations of TEM were performed using a Tecnai G2 F20 S-TWIN operated at 200 KV. Samples of TEM were prepared by double jet electropolishing using an electrolyte consisting of 5 vol.-% perchloric acid and 95 vol.-% ethanol at a temperature below −20°C. The average grain size was determined from TEM dark field images using image analysis software (Photoshop 7·0) to count at least 300 grains for each sample. The post-deformed TEM samples were sampled in the vicinity of tensile fractures.

Dog bone shaped tensile specimens with a gauge length of 10 mm and a gauge width of 3 mm were cut using an electrodischarging machine. Tensile tests were carried out on a CMT-6104 test machine at RT and a strain rate of 10^{-3} s^{-1}. The tensile elongation in the present study was measured through the gripping head movement of the tensile machine.

Results and discussion

The nominal Co content is 75 wt-% determined by EDX. Figure 1 shows the XRD patterns for Ni and the Ni–75%Co alloy. In contrast to Ni, an additional hexagonal close packed (hcp) structure is observed in the Ni–75%Co alloy verifying the presence of a DP structure.

Figure 2 shows engineering stress–strain curves for Ni and the Ni–75%Co alloy. At least two tensile specimens for each metal were tested and the fundamental mechanical properties were concluded in Table 2. The significant increases in the strength and ductility are both seen in the Ni–75%Co alloy in comparison with Ni. The average uniform strain (indicated by short arrows in Fig. 2) and the average ultimate tensile strength are increased by 4·5% and ~400 MPa respectively, from Ni to the Ni–75%Co alloy. When the strain exceeds ~2·6% (beyond the elastic strain), the Ni–75%Co alloy exhibits an evidently higher strain hardening rate than that of Ni, which is shown in the inset of Fig. 2. For NC Ni, an evident coarsening process of shear band was witnessed on the surface of specimen as the tensile stress exceeds the peak value. Subsequently, the crack initiated at the location of shear band and then the specimen was pulled to failure aligning the shear band, ~55° with respect to the tension direction. This is a typical fracture manner for NC metals that are subjected to shear banding plasticity instability.[11,12] Surprisingly, for the NC Ni–75%Co alloy, no shear band was observed on the surface of specimen till the specimen was pulled to failure. Moreover, the Ni–75%Co alloy's fracture was

Table 1 Operating conditions of electrodeposition for producing NC Ni and NC Ni–Co alloy

Parameters	
Electrolyte volume, L	1
Electrolyte temperature, °C	60
pH	3
Average current density, A dm^{-2}	10
On-time in a cycle, ms	50
Duty ratio, %	50
Anode material	Electrolytic Ni (purity > 99·9 wt-%)
Ratio of cathode area to anode area in the plating bath	1 : 4
Cathode substrate	Stainless steel sheet (1Cr15Mn8Ni5Cu2)

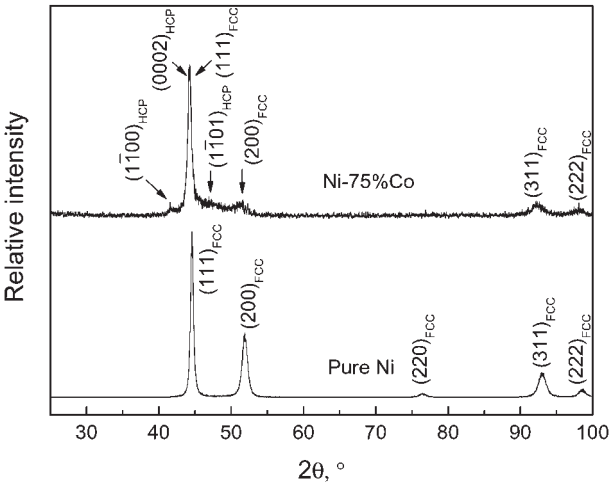

1 X-ray diffraction patterns for Ni and Ni–75%Co alloy

perpendicular to the tensile direction. These together indicate shear banding plasticity instability is strongly suppressed in the Ni–75%Co alloy.

Figure 3*a* shows a typical TEM bright field image of the as deposited Ni–75%Co alloy. It indicates that grains are very uniform and fine, entirely below 20 nm. The average grain size is 7·2 nm with a very narrow distribution of 4–16 nm, which is present in the upper half of Fig. 3*c*. It is well known that Co is a metal with a low stacking fault energy. Therefore, high Co alloys of Ni also generally have a low stacking fault energy with easy nucleation of twins,[18] which was also seen in the present Ni–75%Co alloy. Owing to the absence of nanobeam electron diffraction techniques, the grains from fcc phase or hcp phase fail to be recognisable and thus the quantity and distribution of the two phases fail to be characterised. Compared with Fig. 3*a*, the significant variations of grain size or shape are hardly observed in the post-deformed state, as shown in Fig. 3*b*. But the number of twins is increased in comparison with that observed in the as deposited microstructures. Therefore, deformation twinning is likely to play an important role in the deformation process. Figure 3*c* shows a comparison of grain size statistical distributions before and after deformation. Slight grain growth of <2 nm is obtained by the grain size statistic. In addition, the significant reduction of the number fraction of small grains of 4–6 nm and the slight increase (<3%) of the number fraction of grains of 16–22 nm are exhibited in the post-deformation Ni–75%Co alloy.

Figure 4*a* shows a typical TEM bright field image of the as deposited NC Ni. Apparently, grain sizes of Ni are larger than those of the Ni–75%Co alloy and the grain size distribution is relatively broad in a region of 5–60 nm with the average grain size of 22·4 nm. In the post-deformed Ni sample, as shown in Fig. 4*b*, significant grain growth is observed and even individual large grains with a size up to 120 nm are present. A comparison of grain size statistic of Ni before and after deformation is shown in Fig. 4*c*. It shows that the average grain size increases by 10·4 nm and over 20% of total grains have grown to 40–88 nm after tensile deformation. Similar results were also observed in other electrodeposited NC Ni.[3]

The higher strength in the NC Ni–75%Co alloy in contrast to NC Ni is mainly resulted from grain refinement but maybe less from solid solution strengthening of Ni

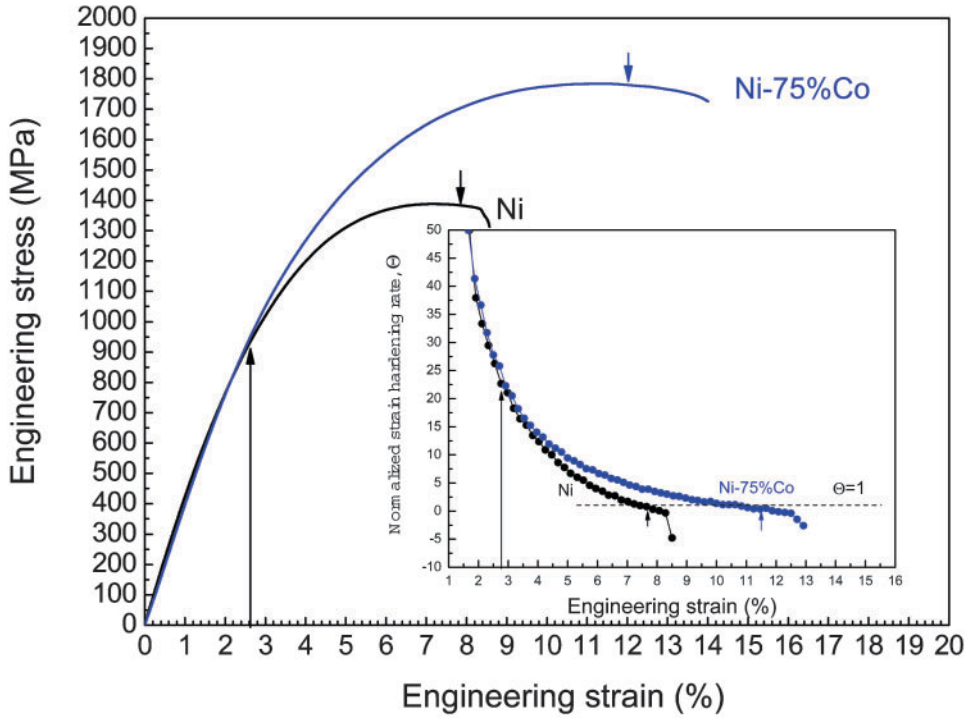

2 Tensile engineering stress σ–strain ε curves for NC Ni and Ni–75%Co alloy: normalised strain hardening rate Θ versus engineering strain ε is shown in inset, where Θ is defined as $\Theta=(d\sigma/d\varepsilon/\sigma)_{\varepsilon}$; short arrows indicate locations of maximum uniform strain

with Co additions due to the nearly identical atomic radius for Ni and Co atoms. In addition, based on the observation of grain structure before and after tensile deformation, a link can be established between the ductility and the degree of stress induced grain growth during tensile deformation. It is confirmed that suppression of grain growth during tensile deformation can delay and even avoid shear banding plastic instability leading to the enhanced uniform strain. A similar example was found in the compressive deformation of an NC Ni–Fe alloy.[19] The compressive strain of the Ni–Fe alloy was enhanced ~6% as grain growth was further suppressed with a decline of deformation temperature from the ambient temperature to the cryogenic temperature.

It is worth noting that the authors' conclusion is in terms of NC metals with free of defects because the tensile specimen is very sensitive to defects inside the specimen, such as pores and brittle inclusions. For example, annealing NC Ni containing the brittle sulphur phase, which is segregating to GBs, can cause a catastrophic failure as the applied stress just exceeds the yielding point.[20] In this case, no grain growth is anticipated because annealing NC Ni is just elastically deformed.

The mechanism for deformation at the nanoscale is grain size dependent. As the grain size is below a critical value (10–15 nm), a transition from dislocation dominated mechanisms to GB dominated mechanisms takes place. Stress induced grain growth has been observed over a range of the grain size spanning 4 to 100 nm in fcc metals by MD simulations or experimental studies.[2–10,14,15] For example, Shan *et al.*[2] prepared a kind of NC Ni with a grain size of ~10 nm, which was below the critical grain size of Ni. The severe stress induced grain coalescence (from 10 to 80 nm) was observed in the *in situ* tensile deformation of this Ni. Although mechanical properties of NC Ni with the grain size below 10 nm are in shortage due to the difficulty in preparation, it is believed that further significantly enhanced ductility in NC Ni with the grain size below 10 nm does not happen since shear banding plastic instability resulted from severe stress induced grain growth fails to be avoided. And the fact is true in NC Ni with the grain size of 6 nm prepared by Wang *et al.*[21] Therefore, the authros think that NC Ni with the grain size as small as the present Ni–75%Co alloy will not show the significantly enhanced ductility in contrast to NC Ni with the grain size of 20–30 nm.

For NC fcc pure metals, grain growth is prone to occur and the propensity has been supported by much experimental evidence.[2–10] However, for NC hcp pure metals, it seems to be an exception. Because negligibly insignificant grain growth was observed in an NC Co metal deformed by cold rolling (24% reduction in the

Table 2 Tensile results of NC Ni and Ni–75%Co alloy

Samples	Yield strength (0·2%), MPa	Ultimate tensile strength, MPa	Elongation to failure, %	Uniform tensile strain, %
Ni	771·3	1385·4	8·5	7·9
	761·5	1371·8	8·9	7·8
Ni–75%Co	1037·1	1786·5	14·0	11·6
	1007·9	1738·2	15·3	13·3

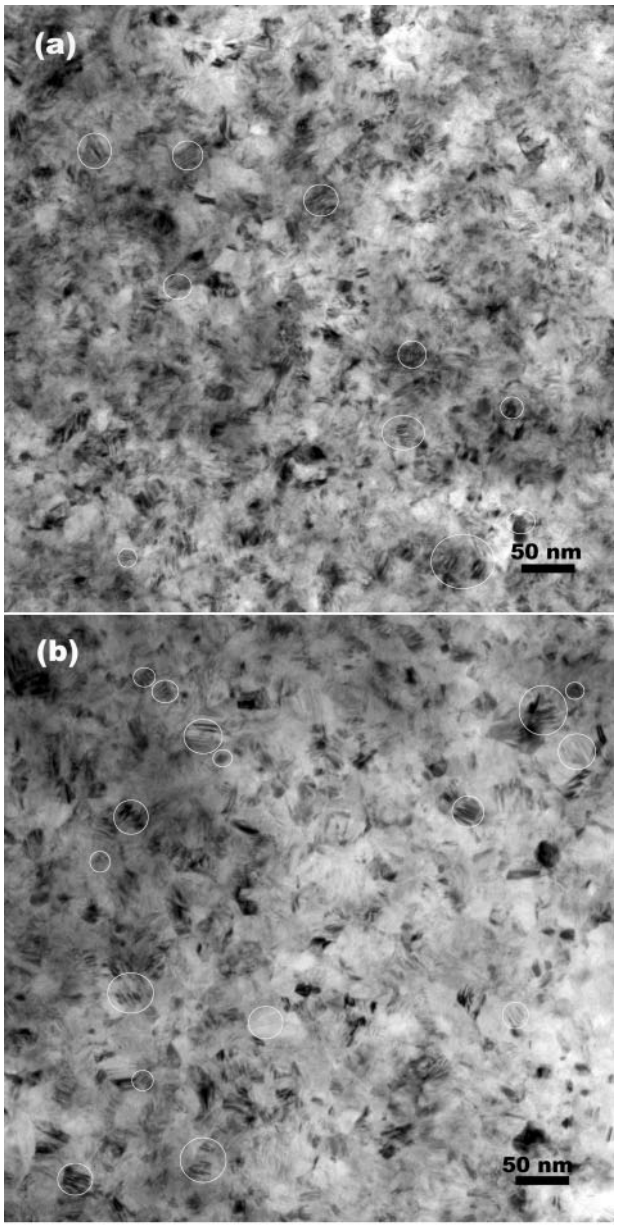

3 Typical TEM images for *a* as deposited and *b* post-deformed NC Ni–75%Co alloy; *c* comparison of grain size statistic before and after deformation

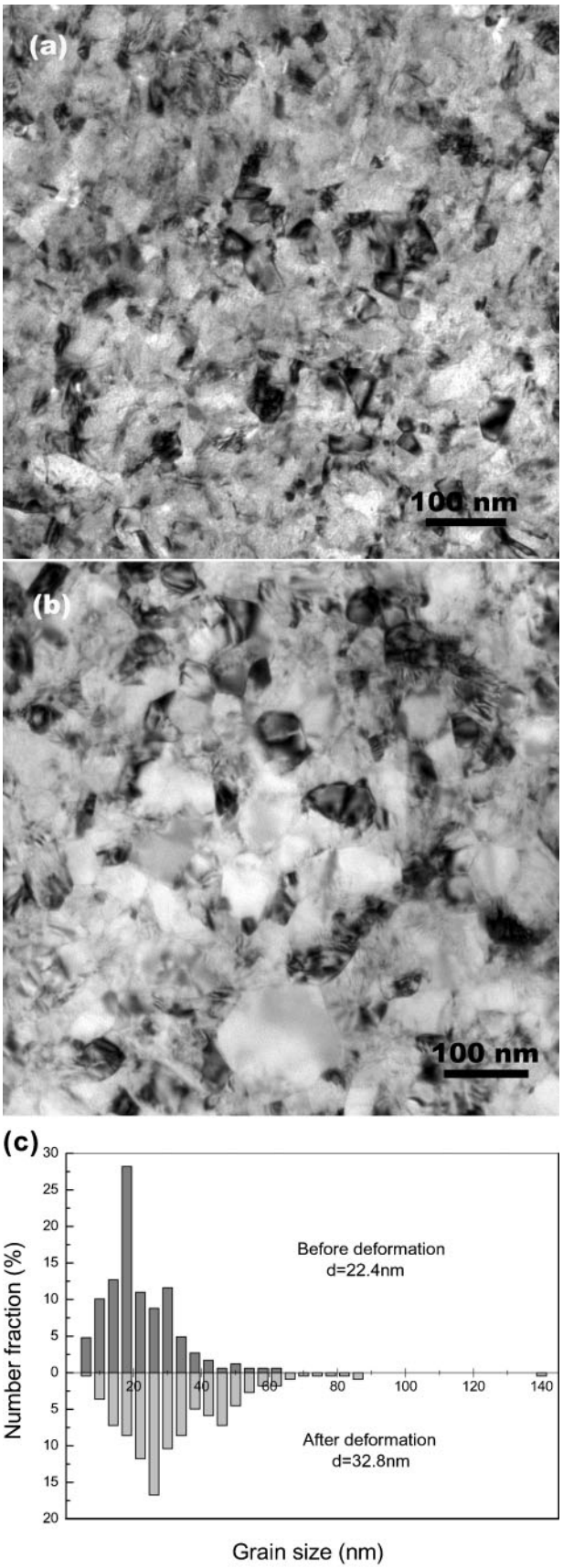

4 Typical TEM images for *a* as deposited and *b* post-deformed NC Ni; *c* comparison of grain size statistic before and after deformation

thickness).[22] This seems to indicate that stress induced grain growth is likely independent of deformation mechanisms but dependent of crystal structures for NC pure metals. Nonetheless, it is considered that the very high ductility obtained in an NC Co metal prepared by Karimpoor *et al.*[23] is also due to complete suppression of grain growth during tensile deformation.

Stress induced grain growth is via GB migration[14,15] or grain rotation.[2,3] Grain boundary migration can be restricted by solutes pinning GB, which has been supported by some examples.[16,19] However, the effect factors as to GB migration capability response to solute atom species and quantity are less understood. Molecular dynamic simulation predicts that second phase segregation to GBs can effectively block GB migration during plastic deformation.[17] In the practical case, the second phase should be ductile, like a metal solid solution, but not a brittle phase, e.g. sulphur and Ni_3P. In addition to blocking GB migration, DP in the nanostructure can assist in preventing formation of grain coalescence induced by grain rotation. For NC pure metals, stress induced grain coalescence is formed by the crystallography reorientation among adjacent grains towards the consistent orientation, which is mediated by grain rotation.[3] It could be conceivable that if grains from a phase are separated by grains from the second phase, grain coalescence would be difficult to create.

At last, twins observed in the deformed Ni–75%Co alloy are to be discussed. In NC metals, deformation twinning is associated with emission of partial dislocations from GBs and is generally activated at higher stresses,[24] e.g. cryogenic tension and rolling.[25,26] Wu and co-workers proposed that in NC metals a majority of deformation twins generate zero contribution to macroscopic strains but mediate deformation via adjusting grain orientations.[26] The critical grain size for the Ni–80%Co alloy in Ref. 18 is 15 nm. Therefore, the present Ni–75%Co alloy with a grain size of 7·2 nm, GB dominated deformation (probably GB sliding) operates in RT tensile deformation. If only GB sliding operates but in the absence of another mechanism to accommodate the strain, it will cause an inevitable stress concentration at the triple points. Subsequently, a void nucleates and quickly grows leading to premature fracture with a low ductility.[27] However, the present Ni–75%Co alloy exhibits a high ductility implying the presence of another operative mechanism. Based on activation of deformation twinning requiring higher stresses in NC regime, it is logical that stress concentrations caused by GB sliding in the Ni–75%Co alloy could be relieved via deformation twinning. Atomistic simulations show stresses in intergranular regions are much higher than in grain interiors.[24] As accumulated stresses in the GB regions reach the needed value for emitting partials, GB partials will be emitted across grain interiors accompanied twins by a 'random activation of partials' mechanism, simultaneously leading to sharp stress relaxations in the GB regions.[24,26] As a result, stress concentrations at the triple points caused by GB sliding are timely relieved, which assists in steady flow deformation gaining a good ductility.

Conclusions

1. An NC DP Ni–75%Co alloy with an average grain size of 7·2 nm and a narrow grain size distribution of 5–15 nm was prepared by pluse electrodeposition.

2. Stress induced grain growth during tensile deformation, even subjected to very high stresses and large strains, is very insignificant for the Ni–75%Co alloy in sharp contrast to the significant stress induced grain growth occurring in Ni.

3. It is proposed that suppression of stress induced grain growth during tensile deformation can delay and even prohibit formation of shear banding plastic instability and then enhances uniform strain leading to the enhanced ductility. The present NC DP Ni–Co alloy is a convincing example.

Acknowledgements

The financial support provided by the Innovation Project of Fuzhou University, the Foundations of Fujian Provincial Natural Science Research Programme (project no. 2008J0145-E0810006) and the National 863 Projects of China (project no. 2007AA03Z325) is gratefully acknowledged.

References

1. U. Klement and M. da Silva: *J. Iron Steel Res. Int.*, 2007, **14**, (5), 173–178.
2. Z. W. Shan, E. A. Stach, J. M. K. Wiezorek, J. A. Knapp, D. M. Follstaedt and S. X. Mao: *Science*, 2004, **305**, 654–657.
3. Y. B. Wang, B. Q. Li, M. L. Sui and S. X. Mao: *Appl. Phys. Lett.*, 2008, **92**, 011903.
4. G. J. Fan, L. F. Fu, H. Choo, P. K. Liaw and N. D. Browning: *Acta Mater.*, 2006, **54**, 4781–4792.
5. G. J. Fan, L. F. Fu, D. C. Qiao, H. Choo, P. K. Liaw and N. D. Browning: *Scr. Mater.*, 2006, **54**, 2137–2141.
6. S. Brandstetter, K. Zhang, A. Escuadro, J. R. Weertman and H. Van Swygenhoven: *Scr. Mater.*, 2008, **58**, 61–64.
7. D. Pan, T. G. Nieh and M. W. Chen: *Appl. Phys. Lett.*, 2006, **88**, 161922.
8. K. Zhang, J. R. Weertman and J. A. Eastman: *Appl. Phys. Lett.*, 2004, **85**, 5197–5199.
9. K. Zhang, J. R. Weertman and J. A. Eastman: *Appl. Phys. Lett.*, 2005, **87**, 061921.
10. X. Z. Liao, A. R. Kilmametov, R. Z. Valiev, H. Gao, X. Li, A. K. Mukherjee, J. F. Bingert and Y. T. Zhu: *Appl. Phys. Lett.*, 2006, **88**, 021909.
11. F. Dalla Torre, H. van Swygenhoven and M. Victoria: *Acta Mater.*, 2002, **50**, 3957–3970.
12. A. Misra, X. Zhang, D. Hammon and R. G. Hoagland: *Acta Mater.*, 2005, **53**, 221–226.
13. Q. Wei, D. Jia, K. T. Ramesh and E. Ma: *Appl. Phys. Lett.*, 2002, **81**, 1240–1242.
14. D. Farkas, A. Froeth and H. van Swygenhoven: *Scr. Mater.*, 2006, **55**, 695–698.
15. J. Schiøtz: *Mater. Sci. Eng. A*, 2004, **A375–377**, 975–979.
16. W. A. Soer, J. Th. M. de Hosson, A. M. Minor, J. W. Morris, Jr and E. A. Stach: *Acta Mater.* 2004, **52**, 5783–5790.
17. D. Farkas, S. Mohanty and J. Monk: *Mater. Sci. Eng. A*, 2008, **A493**, 33–40.
18. B. Y. C. Wu, P. J. Ferreira and C. A. Schuh: *Metall. Mater. Trans. A*, 2004, **36A**, 1927–1936.
19. H. Li, H. Choo and P. K. Liaw: *J. Appl. Phys.*, 2007, **101**, 063536.
20. Y. M. Wang, S. Cheng, Q. M. Wei, E. Ma, T. G. Nieh and A. Hamza: *Scr. Mater.*, 2004, **51**, 1023–1028.
21. N. Wang, Z. Wang, K. T. Aust and U. Erb: *Mater. Sci. Eng. A*, 1996, **A237**, 150–158.
22. X. Zhang and C. Jia: *Mater. Sci. Eng. A*, 2006, **A418**, 77–80.
23. A. A. Karimpoor, U. Erb, K. T. Aust and G. Palumbo: *Scr. Mater.*, 2003, **49**, 651–656.
24. A. G. Froseth, P. M. Derlet and H. van Swygenhoven: *Adv. Eng. Mater.*, 2005, **7**, 16–20.
25. X. Wu, Y. T. Zhu, M. W. Chen and E. Ma: *Scr. Mater.*, 2006, **54**, 1685–1690.
26. X. L. Wu, X. Z. Liao, S. G. Srinivasan, F. Zhou, E. J. Lavernia, R. Z. Valiev and Y. T. Zhu: *Phys. Rev. Lett.*, 2008, **100**, 095701.
27. A. V. Sergueeva, N. A. Mara and A. K. Mukherjee: *Rev. Adv. Mater. Sci.*, 2004, **7**, 67–74.